Journal of Alloys and Compounds, 190 (1992) 129–135
JALCOM 433

Nitrogen gas pressure synthesis and neutron diffraction study of $R_2Fe_{17}N_3$ with R≡Ce and Nd

O. Isnard
Institut Laue-Langevin, BP 156, and Laboratoire de Cristallographie du CNRS, associé à l'Université J. Fourier, 166X, 38042 Grenoble Cédex 9 (France)

S. Miraglia, J. L. Soubeyroux and D. Fruchart
Laboratoire de Cristallographie du CNRS, associé à l'Université J. Fourier, 166X, 38042 Grenoble Cédex 9 (France)

(Received July 21, 1991)

Abstract

A variant synthesis route has been developed using high pressure nitrogen gas, leading to a lower reaction temperature and time and a higher nitrogen content. Here we report on a structural and magnetic study of $Ce_2Fe_{17}N_3$ and $Nd_2Fe_{17}N_3$ synthesized by this method. The compounds have been investigated by means of neutron powder diffraction at 2 and 300 K. The impact of nitrogen insertion on the iron and rare earth magnetic moments is discussed. Finally, enlightening comparisons are made with some iron nitrides (Fe_4N and $Fe_{16}N_2$). The refined site-dependent iron magnetic moments appear to vary significantly with the interatomic distances between iron and nitrogen.

1. Introduction

Many studies have been devoted to investigating the rare earth–transition metal phase diagram; ferromagnetic iron-rich intermetallic compounds are among the most promising hard magnet materials.

So far neither spectroscopy techniques nor neutron diffraction have yielded sufficiently precise sets of the individual iron magnetic moments attached to each of the crystal sites. Since the high nitrogen pressure technique enables one to synthesize fully saturated samples of high crystalline quality, the accuracy of the refinements is improved. Hence, we shall discuss the effect of nitrogen insertion on the local iron magnetic moments.

2. Experimental details

2.1. Synthesis

All the samples were melted in an H.F. induction furnace using the so-called cold-crucible method under an inert atmosphere (argon). The purities of the starting elements were 99.95% for the rare-earth metals and 99.99% for iron. Pieces of the ingots were wrapped into tantalum foil, sealed under argon-filled silica tubes and then annealed for several days at temperatures ranging from 950 to 1050 °C. Standard X-ray diffractometry revealed that the samples were mainly single phase, with the presence of a few traces of α-Fe. Prior to nitrogenation, the starting R_2Fe_{17} alloys were crushed and sieved down to a typical particle size of 20 μm (in diameter).

Unlike previous nitrogenation routes [1–5], here the process has been performed under high pressure, *e.g.* 15 MPa, in a stainless steel autoclave. The purity of the nitrogen (N_2) gas used was 99.9995%. Nitride formation required activation of the binary alloy; this was completed by heating the powder for several hours at a temperature ranging from 250 to 350 °C. A first estimation of the nitrogen uptake was done by a gravimetry method.

2.2. Neutron diffraction experiments

The structural investigations have been carried out using the high flux neutron diffractometer DN5 of the Siloé reactor (Centre d'Etudes Nucléaires de Grenoble) operating at either 2.49 or 1.34 Å. The diffraction data were analysed using the Rietveld technique implemented in the program Fullprof developed at the Institut Laue–Langevin. Figures 1 and 2 represent the diffraction patterns of $Nd_2Fe_{17}N_3$ recorded at 4 K and 300 K respectively. A single overall Debye–Waller parameter was refined, together with the magnetic moments. The

0925-8388/92/$5.00

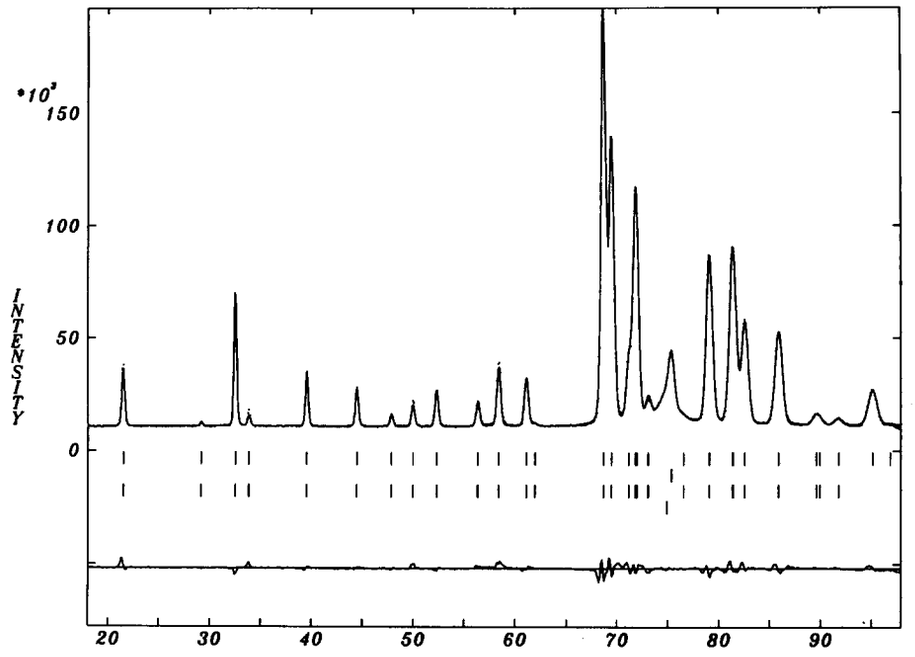

Fig. 1. Neutron powder diffraction patterns of $Nd_2Fe_{17}N_3$ at 4 K recorded with the DN5 diffractometer ($\lambda = 1.34$ Å). The dots and the line refer to the recorded pattern and calculated fit respectively. The difference pattern is plotted in the lower part of the figure. The first and third set of vertical bars refer to the nuclear and magnetic contributions to the diffraction lines of $Nd_2Fe_{17}N_3$. The second set refers to the traces of α-Fe.

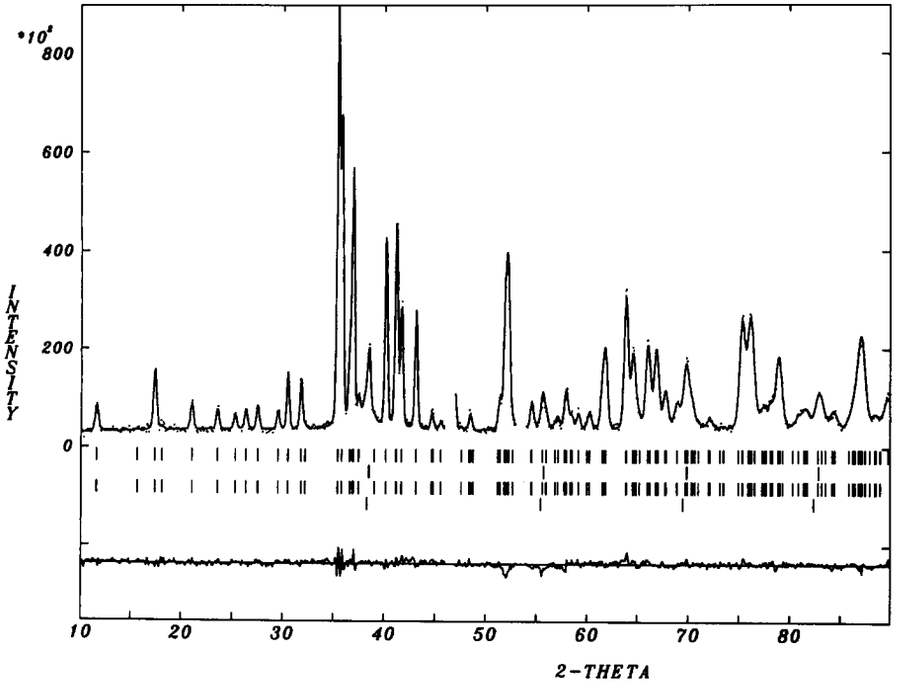

Fig. 2. Neutron powder diffraction patterns of $Nd_2Fe_{17}N_3$ at 300 K recorded with the DN5 diffractometer ($\lambda = 2.49$ Å). The dots and the line refer to the recorded pattern and calculated fit respectively. The difference pattern is plotted in the lower part of the figure. The first and third set of vertical bars refer to the nuclear and magnetic contribution to the diffraction lines of $Nd_2Fe_{17}N_3$. The second set refers to the traces of α-Fe.

neutron scattering lengths used during the refinement of the crystal structure were taken from Sears [6].

Experimental parameters are reported in Table 3.

3. Discussion

3.1. Alloy nitrogenation

In a previous study [7], we have reported an "*in-situ* neutron powder diffraction study of the nitrogenation process of Nd_2Fe_{17}". This chemical reaction can be described by the following reaction:

$$2Nd_2Fe_{17} + 3N_2 \longrightarrow 2R_2Fe_{17}N_3$$

Even at the beginning of the reaction, the resulting nitride particles correspond to a highly charged interstitial phase. Only the relative amounts of the binary host and ternary charged phase have changed, but no major change is observed on their respective compositions. These results are in good agreement with the description in a review paper [8] where Buschow uses the Van't Hoff relation which allows us to define the equilibrium pressure *vs.* ΔH_f and ΔS (the enthalpy and entropy of formation respectively):

$$\ln p_{N_2} = \frac{\Delta H_f}{3RT} - \frac{\Delta S}{3R} \quad (1)$$

In most of the previously reported experiments, the N_2 gas pressure was usually fixed at normal pressure (10^5 Pa). Consequently, the R_2 Fe_{17} alloy began to absorb N_2 gas once the temperature had been raised sufficiently high to overcome the activation energy of the process (a typical reaction temperature is 450–550 °C). Use of a higher N_2 gas pressure enables us to lower the charging temperature, thus leading to higher nitrogen concentrations in the ternary nitrides in agreement with (1).

The experimental nitrogen concentrations reported hereafter, (Tables 1 and 2) are significantly higher than those of Coey and coworkers [1], Ibberson *et al.* [9] or Miraglia *et al.* [4] who found a nitrogen content corresponding to $x = 2.3$, 2.6 and 2.7 nitrogen atoms per formula unit respectively. Most of the papers dealing with the nitrogenation procedure have also pointed out the quasi-systematic occurrence of a disproportionation process leading to the formation of more or less noticeable parts of a rare earth nitride and α-Fe. According to Buschow [8] and Schultz [10], the disproportionation reaction requires a high activation energy since it involves long-range diffusion of metal atoms. Such a metal diffusion can be significantly slowed down and almost avoided when processing at lower temperature. Thus working under a high N_2 pressure and consequently a low temperature could offer two advantages.

(1) A higher nitrogen concentration could be reached (eqn. (1)).

(2) The formation of rare-earth nitride and α-Fe by decreasing the metal atom diffusion rate is not favoured.

These assumptions are confirmed since a very low amount of α-Fe (3 at.% or even less) has been found in both the Ce_2Fe_{17} and the Nd_2Fe_{17} nitrides that we have obtained under pressure. Note that the melting and annealing procedure do not ensure the total absence of residual α-Fe grains in the starting alloy prior to nitrogenation.

3.2. Neutron diffraction analysis

As already mentioned [1, 4], the R_2Fe_{17} nitrides retain the host metal symmetry, and nitrogen insertion leads to an anisotropic lattice expansion which mostly concerns the basal plane of the hexagonal type of cell. The nitrogen atoms fill the 9e sites of the $R\bar{3}m$ space group. These six-coordinated sites have four iron (two in the 18f and two in the 18h position) and two rare earth atoms as nearest neighbours (Fig. 3). Refinement of the stoichiometry leads to 2.95 ± 0.1 nitrogen atoms per formula unit, which is in good agreement with the values of 3 and 2.9, determined by thermogravimetry measurements for Ce_2Fe_{17} and Nd_2Fe_{17} nitrides respectively. This indicates a total occupancy of the 9e interstitial sites, in agreement with the high Curie temperatures measured elsewhere: $T_c = 755$ K for $Ce_2Fe_{17}N_3$ and 770 K for $Nd_2Fe_{17}N_3$.

In recent work Li and Cadogan [11] show that for R_2Fe_{17} nitrides the second-order crystal field term A_2^0 is closely related to the nitrogen concentration. Consequently, using high pressure synthesis which leads to a high nitrogen content, we can expect to reach higher anisotropy field parameters. This would be of particular interest in the case of the Sm_2Fe_{17} nitride, the most promising compound for applications. The lower amount of disproportionated α-Fe seems to be another advantage resulting from this process.

From Table 2, it can be seen that Fe(3)–N and Fe(4)–N bonds in $Nd_2Fe_{17}N_3$ correspond to distances of 1.92 Å and 1.94 Å respectively, close to the shortest Fe–N bond observed in Fe_4N (1.90 Å) and $Fe_{16}N_2$ (1.95 Å). This indicates a strong Fe–N bond as mentioned elsewhere [5].

During the refinement of the magnetic parameters, moments were constrained to be collinear within the basal plane, as expected from the respective signs of the second-order Stevens coefficients α_J and the crystal field parameter A_2^0. In the case of the cerium compounds, no magnetic moment has been found on the R atoms. However, at low temperatures, owing to the relative weakness of the magnetic contributions, only an average iron magnetic moment has been refined for $Nd_2Fe_{17}N_3$. Comparison of the magnetic moments listed in Tables

TABLE 1. Refined structural parameters for $Ce_2Fe_{17}N_3$; at $T=4$ K the B values were fixed to 0

T (K)	Atom	Site	x	y	z	n	m (μ_B)	B (Å^2)
4	Ce	6c	0	0	0.3408(24)	0.1667	–	
4	Fe(1)	6c	0	0	0.0973(8)	0.1667	3.18(16)	
4	Fe(2)	9d	0.5	0	0.5	0.25	2.64(15)	
4	Fe(3)	18f	0.2818(7)	0	0	0.5	2.15(12)	
4	Fe(4)	18h	0.5043(4)	0.4957(4)	0.1537(5)	0.5	2.01(12)	
4	N	9e	0.5	0	0	0.248(3)	–	
300	Ce	6c	0	0	0.3425(25)	0.1667	–	0.5
300	Fe(1)	6c	0	0	0.0963(8)	0.1667	2.93(18)	0.5
300	Fe(2)	9d	0.5	0	0.5	0.25	2.34(17)	0.5
300	Fe(3)	18f	0.2793(6)	0	0	0.5	1.85(15)	0.5
300	Fe(4)	18h	0.5049(4)	0.4951(4)	0.1537(5)	0.5	1.71(14)	0.5
300	N	9e	0.5	0	0	0.248(3)	–	0.8

TABLE 2. Refined structural parameters for $Ce_2Fe_{17}N_3$; at $T=4$ K the B values were fixed to 0

T (K)	Atom	Site	x	y	z	n	m (μ_B)	B (Å^2)
4	Nd	6c	0	0	0.3409(7)	0.1667	3.80(20)	
4	Fe(1)	6c	0	0	0.0941(4)	0.1667	3.40(20)	
4	Fe(2)	9d	0.5	0	0.5	0.25	2.13(17)	
4	Fe(3)	18f	0.2821(3)	0	0	0.5	2.22(15)	
4	Fe(4)	18h	0.5056(2)	0.4944(2)	0.1526(2)	0.5	1.91(14)	
4	N	9e	0.5	0	0	0.246(2)	–	
300	N(d)	6c	0	0	0.3437(5)	0.1667	1.79(1)	0.65(14)
300	Fe(1)	6c	0	0	0.0922(3)	0.1667	2.80(11)	0.65(14)
300	Fe(2)	9d	0.5	0	0.5	0.25	1.93(12)	0.65(14)
300	Fe(3)	18f	0.2814(2)	0	0	0.5	1.93(12)	0.65(14)
300	Fe(4)	18h	0.5057(1)	0.4943(1)	0.1531(3)	0.5	1.93(12)	0.65(14)
300	N	9e	0.5	0	0	0.246(2)	–	0.8

1 and 2 for $Ce_2Fe_{17}N_3$ and $Nd_2Fe_{17}N_3$ respectively reveals some similarities. In both cases the refined iron magnetic moments are found to be fairly dependent on the crystal site. At 4 K, a wide range of magnitude is observed for the iron moment from 1.9 μ_B to about 3.2 μ_B for both compounds. This dispersion range is also observed at room temperature. In $Ce_2Fe_{17}N_3$, as in $Nd_2Fe_{17}N_3$, the largest iron moment is observed on the dumbbell site with values of around 3 μ_B (at 4 K). The Fe(3) and Fe(4) sites exhibit the lowest iron moment encountered in these compounds (about 2 μ_B). Larger magnetic moments on the dumbbell site have also been observed for $Nd_2Fe_{17}H_5$, as already reported in a previous study [12]. The room-temperature magnetic moments obtained for $Nd_2Fe_{17}N_3$ are close to those found for $Nd_2Fe_{17}H_5$ [12] but, at 4 K, $Nd_2Fe_{17}N_3$ exhibits larger magnetic moments than $Nd_2Fe_{17}H_5$, especially on the neodymium site. A site dependence of the iron local magnetic moment has already been observed for the $Th_2Fe_{17}C_x$ compounds [13]. Furthermore the magnitude of the magnetic moment found in each site of $Th_2Fe_{17}C_x$ is the same as that obtained on the R_2Fe_{17} nitrides. Carbon and nitrogen seem to have the same microscopic effect on the local iron magnetic moments. As shown in Table 4, the order of magnitude of the iron magnetic moment refined for $Ce_2Fe_{17}N_3$ well agrees with the calculation of Li *et al.* [14] performed for $Y_2Fe_{17}N_3$, but the experimental local moments are not exactly the same as the calculated values. Li *et al.* have obtained moments slightly larger for the nitrogen nearest-neighbour iron sites (sites 18f and 18h for $Ce_2Fe_{17}N_3$) than those calculated on the corresponding site in $Y_2Fe_{17}N_3$ (Table 4). The discrepancy can be due to (1) the difference in the rare earth metal (cerium instead of yttrium), (2) the approximations made in the model of Li *et al.* or (3) the fact that neutron diffraction is only sensitive to local magnetism.

The lowest magnetic moments (1.8 μ_B in $Ce_2Fe_{17}N_3$ at room temperature) are refined for the 18f and 18h iron sites which are both the nearest neighbours of nitrogen at distances of 1.91 Å and 1.96 Å respectively (see Fig. 3). The dumbbell site exhibits the largest magnetic moment (2.9 μ_B in $Ce_2Fe_{17}N_3$ at 300 K) and is the farthest of the iron neighbours of the nitrogen

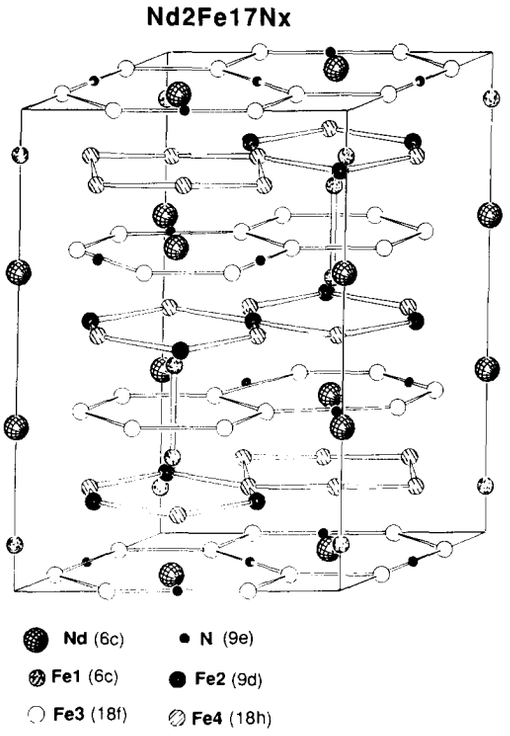

Fig. 3. Crystal structure of $Nd_2Fe_{17}N_3$.

atom: $d_{Fe(1)-N}=3.92$ Å. The moment on the 9d site (Fe(2)) is 2.34 μ_B and it corresponds to a distance of 3.29 Å to nitrogen atoms. The iron magnetic moment seems to be closely related to the interatomic Fe–N distances; the shorter the distances, the lower are the magnetic moments:

$$d_{Fe(1)-N} > d_{Fe(2)-N} > d_{Fe(3)-N} \approx d_{Fe(4)-N}$$

$$m_{Fe(1)} > m_{Fe(2)} > m_{Fe(3)} \approx m_{Fe(4)}$$

To summarize this, it must be noticed that nitrogen insertion in R_2Fe_{17} has macroscopic effects such as raising both the saturation magnetization and the Curie temperature. In addition to this magnetovolumic effect [8], nitrogen insertion leads to lower magnetic moments of its nearest neighbours 18f and 18h and to higher moments on the farthest iron.

So, a wide range of magnetic moments has been observed depending on the iron site and the Fe–N distance. However, the rise in Curie temperature appears far larger than could be expected from the increase in magnetization based on a molecular field model.

3.3. Comparison with the iron nitrides

Since the early work of Jack [15, 16] on the Fe–N system and the discovery of $Fe_{16}N_2$, much work has been devoted to the iron nitrides Fe_4N, $Fe_{16}N_2$ etc. [17–27]. In their model, Wiegner and Berger [17] have considered nitrogen as an electron donor, leading to 3 μ_B and 2 μ_B for the two different iron sites in Fe_4N [17]. The model of Zener [18] considered nitrogen as an acceptor. Using neutron diffraction, Frazer [19] has refined a moment of 2.98 μ_B for iron situated at the corner of the cell whereas iron located at the centre of the face shared only 2.01 μ_B. The magnitude of the moments appeared in agreement with that predicted by Wiener and Berger; however, Frazer concluded that the corresponding model of transferred charge was no longer valid. Later Elliott [20] has proposed a covalent bond picture between nitrogen and iron in Fe_4N, and more recently Zhou *et al.* [21] have described a unified model in which the N 2p and Fe 4s orbitals of nearest iron atoms have strong interactions, whereas the 3d bonds remain almost the same as in the pure iron metal [21].

It should be noted that in Fe_4N, $Fe_{16}N_2$ and $R_2Fe_{17}N_3$ compounds the nitrogen atoms are located in octahedral sites surrounded by six metal atoms (Fig. 3), the shortest Fe–N distance being around 1.90 Å. As shown in Table 4, the three nitrides exhibit in common a wide range of magnetic moments depending on the considered iron sites and the Fe–N distances. The largest magnetic moment of around 3 μ_B is found for the farthest nitrogen neighbours, whereas the lowest moment is around 2 μ_B in all these nitrides and is observed with the nearest nitrogen neighbours. Several workers have demonstrated such a wide range of local magnetic moments in Fe_4N and $Fe_{16}N_2$ using neutron diffraction or Mössbauer experiment. Sugita *et al.* [22] emphasized that the origin of giant magnetization of $Fe_{16}N_2$ is not yet clear. The

TABLE 3. Lattice parameters and reliability factors from the $Ce_2Fe_{17}N_3$ and $Nd_2Fe_{17}N_3$ structure refinements: the agreement factors are the conventional Rietveld factors R_{expt}, R_p, R_B and R_M which refer to the expected, profile, Bragg and magnetic factors respectively; λ is the neutron wavelength used

Compound	λ (Å)	T (K)	a (Å)	c (Å)	V (Å^3)	R_{expt} (%)	R_p (%)	R_B (%)	R_M (%)
$Ce_2Fe_{17}N_3$	2.49	4	8.727(1)	12.687(1)	836	1.57	9.53	5.38	7.61
$Ce_2Fe_{17}N_3$	2.49	300	8.737(1)	12.702(1)	839	3.04	10.9	5.74	7.21
$Nd_2Fe_{17}N_3$	1.34	4	8.750(1)	12.626(1)	837	1.60	8.42	3.11	3.57
$Nd_2Fe_{17}N_3$	2.49	300	8.786(1)	12.676(1)	847	1.24	5.74	2.56	3.16

TABLE 4. Interatomic Fe–N distances and local magnetic moments on the iron sites for $Ce_2Fe_{17}N_3$, Fe_4N and $Fe_{16}N_2$

Compound	Iron site	Fe–N (Å)	Magnetic moment (μ_B)	
			Observed	Calculated
$Ce_2Fe_{17}N_3$	6c	3.92	2.92(18)[a]	2.96[b]
	9d	3.29	2.34(17)[a]	1.78[b]
	18f	1.91	1.85(15)[a]	2.14[b]
	18h	1.96	1.71(14)[a]	2.23[b]
Fe_4N	3c	1.90	2.0[c] to 2.01[d]	2.03[e]
	1a	3.29	3.0[c] to 2.86[d]	3.07[e]
$Fe_{16}N_2$	4d	3.26	–	2.91[f] to 2.83[e]
	4e	1.95	–	1.96[f] to 2.27[e]
	8h	2.02	–	2.28[f] to 2.25[e]

[a]This work.
[b]Calculation for $\frac{1}{2}Y_2Fe_{17}N_3$ of Li *et al.* [14].
[c]Mössbauer spectroscopy study of Shirane *et al.* [25].
[d]Neutron diffraction study of Frazer [19].
[e]Data from Sokuma [23].
[f]Data from Ishida *et al.* [26].

self-consistent calculations of the electronic structures of Fe_3N, Fe_4N and $Fe_{16}N_2$ carried out by Sokuma [23] provide several pieces of information on the effect of nitrogen in iron nitrides.

(1) The insertion of nitrogen atoms has enormous influence on the magnetic moments, raising the macroscopic magnetization.

(2) The large change in the iron local moment is caused by the nitrogen atom through the direct Fe–N bonding.

We have observed similar behaviour for the $R_2Fe_{17}N_3$ series of compounds (see Section 3.2).

The degree of hybridization with nitrogen seems to be a determining factor for the magnetic polarisation of the iron atoms in R_2Fe_{17} nitrides as well as in Fe_4N and $Fe_{16}N_2$. As a conclusion, the $R_2Fe_{17}N_3$ compounds show many features in common with iron nitrides (Table 4): (1) the magnitude of the iron magnetic moments; (2) the similar Fe–N bond distances (the same shortest Fe–N distances, *e.g.* 1.9 Å); (3) the wide range of magnetic moments depending on the iron sites; (4) the large magnetovolumic effect due to nitrogen insertion.

4. Conclusion

An alternative route has been developed using high pressure nitrogen gas to synthesize R_2Fe_{17} nitrides. This offers the advantages of lowering the reaction temperature and obtaining a higher nitrogen content, without the formation of a significant amount of free iron particles. This technique should enable one to attain maximized magnetic properties (anisotropy field, Curie temperature etc.). Neutron diffraction refinements confirm the high nitrogen concentration leading to the formula $R_2Fe_{17}N_{2.9\pm0.1}$. The refined site-dependent iron moments vary significantly with the interatomic distances between iron and nitrogen. The magnitudes of the local iron moments are very similar to those encountered in binary iron nitrides, *e.g.* Fe_4N and $Fe_{16}N_2$.

Apart from the already-reported large influence on the exchange interactions and on the magnetocrystalline parameters, it is revealed that nitrogen insertion has two other effects: firstly it increases the net magnetization; secondly it decreases that of the closest iron neighbours to about (1.7–2) μ_B and yields higher moments on the farthest iron sites (3 μ_B).

Acknowledgment

The authors thank the Département de Recherches Fondamentales du Centre d'Etudes Nucléaires de Grenoble for providing us with the neutron scattering facilities.

References

1 H. Sun, J. M. D. Coey, Y. Otani and D. P. F. Hurley, *J. Phys.: Condens. Mater.*, *2* (1990) 6465.
2 O. Isnard, S. Miraglia, J. L. Soubeyroux, D. Fruchart and A. Stergiou, *J. Less-Common Met.*, *102* (1990) 273.
3 K. H. J. Buschow, T. H. Jacobs and W. Coene, *IEEE Trans. Mag.*, *26* (1990) 1364.
4 S. Miraglia, J. L. Soubeyroux, C. Kolbeck, O. Isnard, D. Fruchart and M. Guillot, *J. Less-Common Met.*, *171* (1991) 57.

5 O. Isnard, S. Miraglia, J. L. Soubeyroux and D. Fruchart, *Phys. Rev. B, 45* (1992) 2920.
6 V. F. Sears, *Internal Rep. AECL 8490,* 1984 (Chalk River Nuclear Laboratory, Atomic Energy of Canada Ltd.).
7 O. Isnard, J. L. Soubeyroux, S. Miraglia, D. Fruchart, L. M. Garcia and J. Bartolomé, *Physica B., 180/181* (1992) 629.
8 K. H. J. Buschow, *Rep. Prog. Phys., 54* (1991) 1123.
9 R. M. Ibberson, O. Moze, T. H. Jacobs and K. H. J. Buschow, *J. Phys.: Condens. Mater., 3* (1991) 1219.
10 L. Schutz, personal communication, 1991.
11 H. S. Li and J. M. Cadogan, *Solid State Commun., 80* (1991) 905.
12 O. Isnard, S. Miraglia, J. L. Soubeyroux and D. Fruchart, *Solid State Commun., 81* (1) (1992) 13.
13 O. Isnard, J. L. Soubeyroux, D. Fruchart, T. H. Jacobs and K. H. J. Buschow, *J. Alloys Comp., 186* (1992) 135.
14 L. P. Li, H. S. Li and J. M. D. Coey, *Phys. Status Solidi, 166* (1991) K107.
15 K. H. Jack, *Proc. R. Soc. London, Ser. A, 208* (1951) 200.
16 K. H. Jack, *Proc. R. Soc. London, Ser A, 208* (1951) 216.
17 G. W. Wiegner and J. A. Berger, *J. Met., 7* (1955) 360.
18 C. Zener, *Phys. Rev., 75* (1952) 324.
19 B. C. Frazer, *Phys. Rev. B, 129* (1958) 751.
20 N. Elliott, *Phys. Rev. B, 129* (1963) 1120.
21 W. Zhou, L. Qu, Q. M. Zhang and D. S. Wang, *Phys. Rev. B, 40* (1989) 6393.
22 Y. Sugita, K. Mitsuaka, M. Komuro, H. Hoshiya, Y. Kozono and M. Hanozono, *J. Appl. Phys., 70* (1991) 5977.
23 A. Sokuma, *J. Magn. Magn. Mater., 102* (1991) 127.
24 A. J. Nozik, J. C. Wood, Jr., and G. Haacke, *Solid State Commun., 7* (1969) 1679.
25 G. Shirane, W. J. Kakei and S. L. Ruby, *Phys. Rev., 126* (1962) 49.
26 S. Ishida, K. Kitawatase, S. Fujii and S. Asano, *J. Phys.: Condens. Matter., 4* (1992) 756.
27 K. Nakajima, T. Yamashita, M. Takata and S. Okamoto, *J. Appl. Phys., 70* (1991) 6033.